# Study of structural and electronic properties of intercalated CrTiS$_2$ compound by density functional theory

V.B. Parmar, A.M. Vora$^*$

Department of Physics, University School of Sciences,

Gujarat University, Navrangpura, Ahmedabad 380009, Gujarat, India

E-mail: voraam@gmail.com

In the present paper, we report the structural optimization of intercalated CrTiS$_2$ compound by using Density Functional Theory (DFT) with Generalized Gradient Approximation (GGA) through Quantum ESPRESSO code. All the computations are carried out by using an ultra-soft pseudopotential. The effect of charge transfer from guest 3d transition metal Cr-atom to self-intercalated compound TiS$_2$ has been studied. In electronic properties, the energy band structure, total density of states (TDOS), partial density of states (PDOS) and Fermi surface have carried out. From the energy band structure, we conclude that the TiS$_2$-intercalated compound has a small bandgap while the doped compound with guest Cr-atom has metallic behavior as shown form its overlapped band structure.

**Keywords:** Density Functional Theory (DFT), Generalized Gradient Approximation (GGA), intercalated compound, density of states, energy band structre, Fermi surface.

## Introduction

The study of structural and electronic properties of material gives a basic understanding of the material. The intercalated compound Titanium sulphide (TiS$_2$) has been developed by transition metal general formula TX$_2$ [1]. The Coulomb interaction has an important in 3d state of transition metal sulphide TiS$_2$, because of it will improve the electronic property of TiS$_2$. Strong covalent bonding in

$TiS_2$ has existed due to the strong hybridization in Ti (3d-state) and S (3p-state). In $TiS_2$, the Ti has a sandwiched layer between two sulphur layers. The outer sulphur and adjacent sulphur layers are weakly connected with the van der Walls forces. It has a very small indirect bandgap or semi-metallic ground state then it has a semiconductor. In very weak van der Walls attraction between interlayer then guest atom can be easily intercalated in pure $TiS_2$. Guest atom Cr has intercalated with transition metal $TiS_2$, when strong hybridization occurs in Cr-3d, Ti-3d and S-3p states. While, X-ray Photoemission Spectroscopy (XPS), Angle Resolved Resonant Photoemission Spectroscopy (ARPES), Angle Resolved Inverse Photoemission Spectroscopy (ARIPES) and high field magnetization measurements proved this conclusion by experimentally [2-6]. We concluded that the electronic properties of $CrTiS_2$ have depended on the guest atom like Cr. Very recently, the Density Functional Theory (DFT) based construction is usually used for examining the structural and electronic properties of the materials and found successful [7-11]. Similarly from the calculation, d-orbitals of intercalant M-atoms hybridize strongly with s-orbitals. Such that the above calculation says Cr-S bonds stronger than the Ti-S bonds [12].

## Computational Aspects

The computations in $CrTiS_2$ compound are calculated with the computational code Quantum ESPRESSO [13]. In $CrTiS_2$ the structural optimization and electronic properties such as band structure, density of states, partial density of states, Fermi surfaces and charge density are calculated by using Generalized Gradient Approximation (GGA) [14]. In the present computation, we have used Perdew-Burke-Ernzerhof (PBE) [15] with ultra-soft pseudopotential [16]. To plot the optimization curve and energy band structure, we have utilized gnuplot [17, 18] while for the plots of density of states (DOS), partial or projected density of states (PDOS), total density of states (TDOS), Fermi surfaces and charge density, we have used XCrySDen [19].

## Results and discussion

In the present section, the spatial attention is drawn about our computationally generated results of said materials.

*Structural optimization*

The structural properties are visualized by the lattice constant. The $TiS_2$ has the $CdI_2$-type layer structure. In which, the Ti layer is sandwiched in two sulfur layers. The structure of $TiS_2$ is shown in Figure 1(a). In this structure, the unit cell of $TiS_2$ contains six atoms. In the unit cell position for Ti is a 1a; the two S atoms are positioned in 2d (1/3, 1/3, 0.2501) and (2/3, 1/3, -0.2501), repectively. The $TiS_2$ has a lattice parameters a=3.4285 and c=5.8944. The structure consists of S-Ti-S sandwiches, separated in the z-direction by the van der Walls gap [20]. Because of very weak van der Walls attraction between the Ti and S layers, the $TiS_2$ can be easily doped by Cr atom. The lattice position of Cr atom is 1b (0,

0, 0.5) in the structure. The struture of $CrTiS_2$ has a hexagonal type with space group $P\bar{3}ml$ [164] as shown in Figure 2. It has lattice parameters a=3.4395 and c=5.9303. The Brillouin zone (IBZ) for the hexagonal structure as shown in Figure 3. The optimizations of lattice parameters are performed for Titanium Disulphide $(TiS_2)$ and Chromium Titanium Disulphide $(CrTiS_2)$. For the relaxation of ground state geometry, three main steps are carried out [21].

1. Convergence of total energy with respect to kinetic energy up to an accuracy of $10^{-4}$ Ry.

2. Convergence of total energy versus $k$-mesh accuracy of $10^{-4}$ Ry.

3. Optimization of lattice constants to minimize the total energy.

After this, the ratio of lattice parameters (c/a) was optimized to verify the results by using the GGA approach with ultra-soft pseudopotential. In Table 1 the computed results of lattice parameters are presented. The optimization curves for $TiS_2$ and $CrTiS_2$ are shown in Figure 4 and Figure 5.

Table 1.
Calculated lattice parameters for $TiS_2$ and $CrTiS_2$.

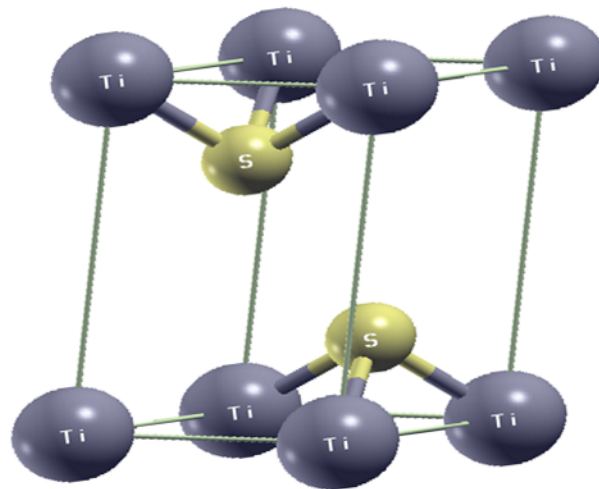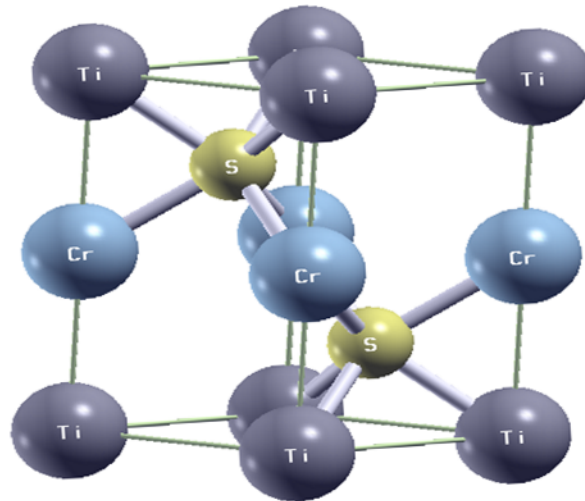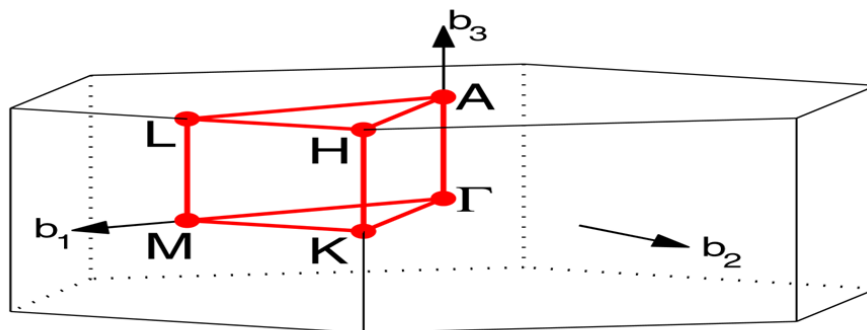| System | Code | Approximation | Lattice Constants (Å) |
|---|---|---|---|
| $TiS_2$ | QE | GGA | a=3.4285 c/a=1.7245 |
| $CrTiS_2$ | QE | GGA | a=3.4395 c/a=1.7236 |



Figure 1. Crystal structure of $TiS_2$.

*Electronic properties*

In electronic properties, we have computed the energy band structure, density of states (DOS), total density of states (TDOS), partial or projected density of states (PDOS) and Fermi surfaces with using Density Functional Theory (DFT) with Generalized Gradient Approximation (GGA) through Quantum ESPRESSO code [13].
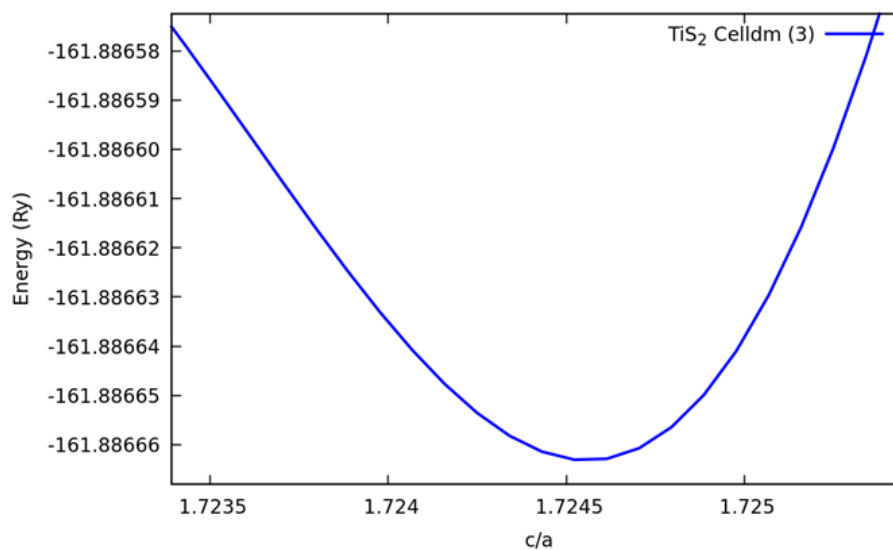
*Band structure*

For a crystalline material, a two dimensional representation of energy of the crystal orbital is called band structure. In this work, the band structures of $TiS_2$ and $CrTiS_2$ compounds are plotted using the gnuplot displayed in Figure 6 and Figure 7, respectively. In both cases, the $k$-points path is considered on the high
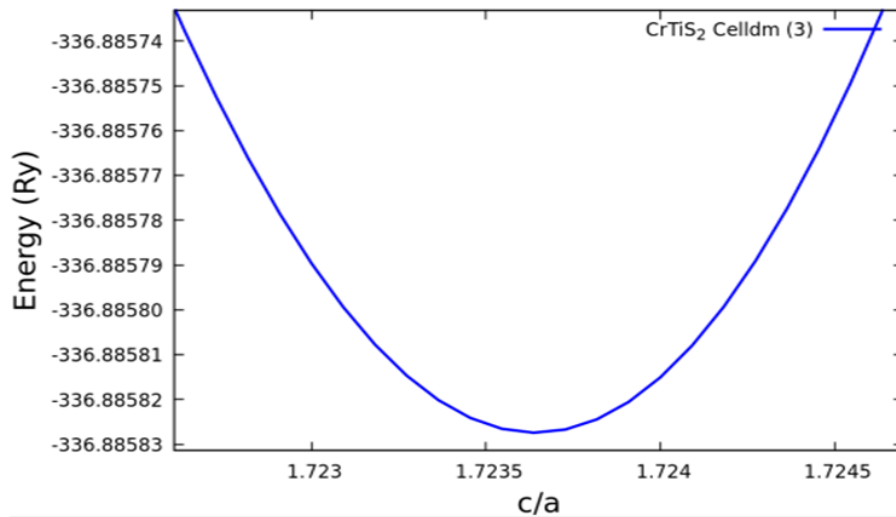
Figure 2. Crystal Structure of CrTiS $_2$.



HEX path: Γ–M–K–Γ–A–L–H–A|L–M|K–H

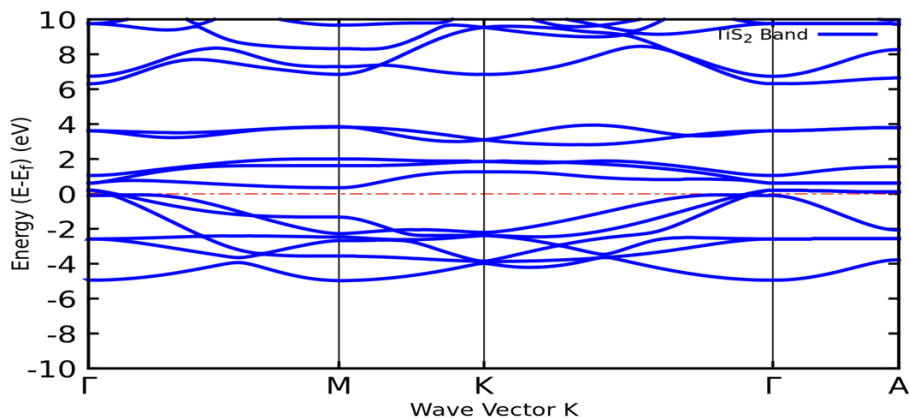Figure 3. Brillouin zone for Hexagonal structure.



Figure 4. Optimization curve for TiS $_2$.

symmetry points, $k$-path. In band structure of both TiS$_2$ and CrTiS$_2$, $k$-point is
$\Gamma \rightarrow M \rightarrow K \rightarrow \Gamma \rightarrow A$. For both TiS$_2$ and CrTiS$_2$ compounds, the kinetic energy
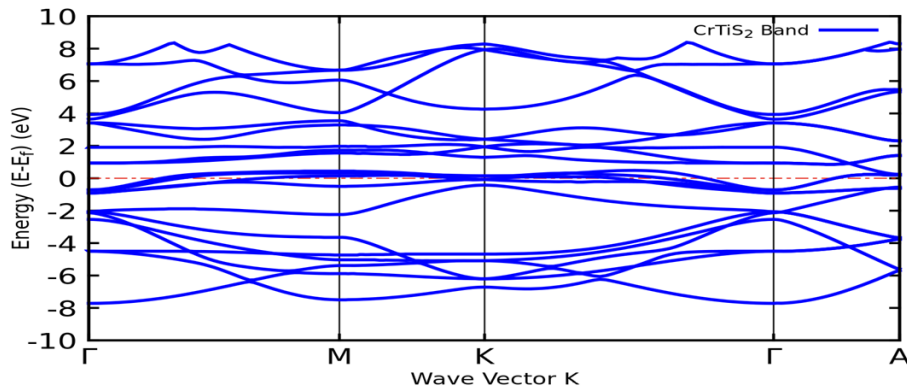cutoff 80 Ry and charge density cutoff 320 are taken. A $k$ mesh of $12 \times 12 \times 12$ is

Figure 5. Optimization curve for CrTiS$_2$.

taken on the calculated $k$-point by the GGA approach.

The energy band structures of TiS$_2$ shown in Figure 6 have been plotted in the energy range -10.0 eV to 10.0 eV. The $k$-path of the band structure is high symmetry directions with the irreducible Brillouin zone (IBZ). In the TiS$_2$ band structure, it is cleared that TiS$_2$ has a semiconductor characteristic, as a small indirect bandgap [6, 21]. From Figure 6, the valance band lines over the Fermi energy but not overlap. Same type of the band structure of CrTiS$_2$ as shown in Figure 7, it is cleared that the CrTiS$_2$ has a metallic characteristic, as overlapping of band lines near the Fermi region is seen. In CrTiS$_2$, the spin component is added for the computation. Band structures for up spin and down spin are plotted. From Figure 7 the valance band and the conduction band are overlapped in the energy range -2.5 eV to 2.5 eV. Above this, we have concluded that the intercalated compound TiS$_2$ has a semiconductor characteristic, while the Cr atom has doped than CrTiS$_2$ has a metallic characteristic. In CrTiS$_2$, the band is overlapped maximum at the Fermi level.



Figure 6. Electronic band structure of TiS$_2$.

In the present work, we observe that the TiS$_2$ has an indirect bandgap or semi metallic ground state while in CrTiS$_2$, the energy bands are overlapped. It is because of doped Cr atom. However, the chromium is a paramagnetic material in nature. Because of it CrTiS$_2$ has a paramagnetic material. The spin up and spin

Figure 7. Electronic band structure of CrTiS $_2$.

down in the band structure of CrTiS2 are having the same nature in the present computation. Hence, only one band structure is shown [12].

*Density of states*

The number of available energy states, per unit energy per unit volume is the density of states (DOS). From the partial or projected DOS, the contributions from the individual orbitals of different materials, like s, p, d and f, can be checked [6].We have used the tetrahedral method for integration over the Brillouin zone is used to estimate the DOS.

Figure 8 and Figure 9, show the TDOS and PDOS for TiS $_2$. It is plotted in the energy range between -20.0 eV to 5.0 eV. The electron density of about zero states/eV is observed below the Fermi region at -10.0 eV. The density of states of TiS $_2$ maximum at -5.0 eV to 0.0 eV. The electron density is of zero states/eV, at the Fermi level. In this, the S 2p-states strongly hybridize with Ti 3d-states. At the Fermi energy level, Ti 3d-states mainly contribute to the conduction band, where the S 2p-states contribute mainly to the valance band [8]. The PDOS of TiS $_2$, we have calculated the electron unfilled states, likewise Ti 3d and S 2p-states. In Figure 9, the PDOS of Ti 3d maximum contributes in the conduction band range 0.0 eV to 5.0 eV where S 2p maximum contributes in the valance band range-5.0 eV to 0.0 eV. Since the Cr atom is doped between sulphur layers. In CrTiS $_2$, the strong hybridization is seen between Cr 3d- and S 3p-states, also weak hybridization is observed between Ti 3d- and S 3p-states.
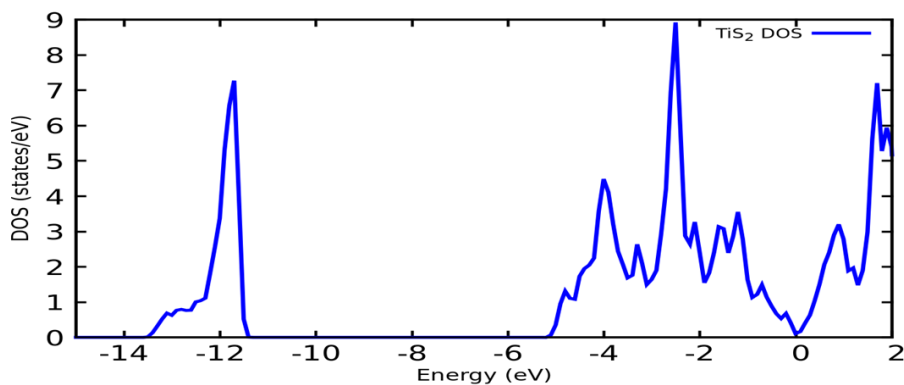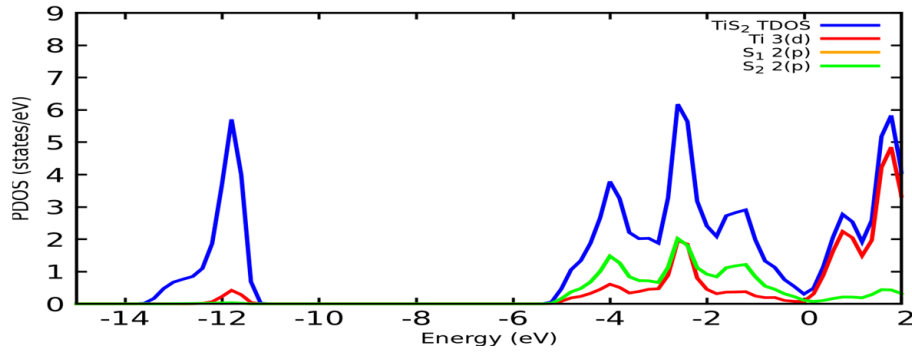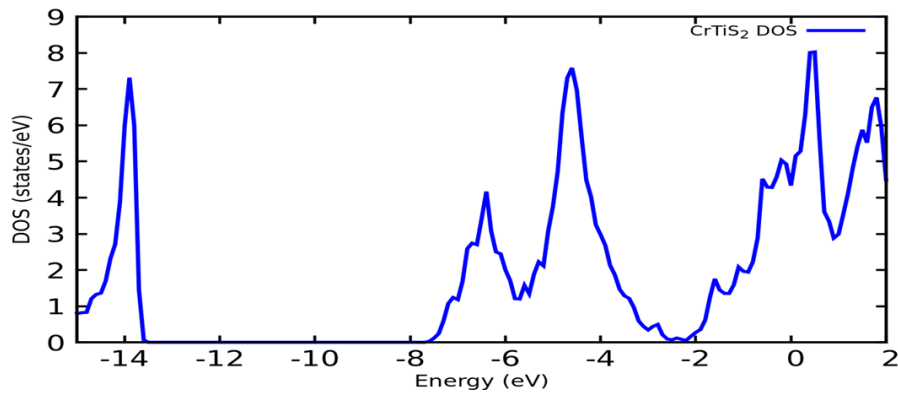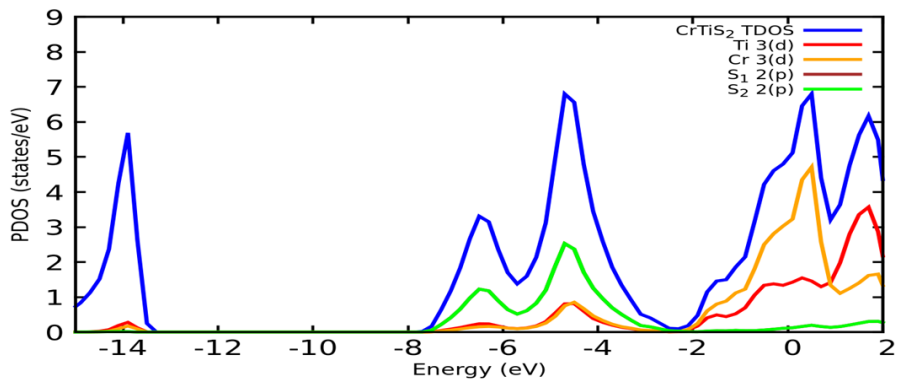


Figure 8. Total DOS of TiS $_2$.

Figure 10 and Figure 11 show the TDOS and PDOS for CrTiS $_2$ compound. It is plotted in the energy range between -25.0 eV to 10.0 eV. In TDOS below the

Figure 9. PDOS for TiS$_2$.

Fermi region, the electron density maximum at 7.5 states/eV at a point -5.0 eV and above the Fermi region the electron density maximum at 6.8 states/eV at a point 2.0 eV. The density of states at the Fermi region is 8.1 states/eV. We show that at the Fermi region the density of states is maximum, because of the band overlapping. In PDOS of CrTiS$_2$ is drawn in the states of Cr 3d, Ti 3d and S 2p-states. In PDOS, the Cr 3d and Ti 3d-states are mainly contributing to the conduction band, while S 2p-states mainly contributes to the valance band. At the Fermi region, the Cr is maximum. We conclude that the CrTiS$_2$ has a metallic material.



Figure 10. Total DOS of CrTiS$_2$.



Figure 11. Total DOS of CrTiS$_2$.

*The Fermi surfaces*

The Fermi energy is the characteristic energy that distinguishes between the occupied and unoccupied energy levels. It is the concept that helps us to picture

the relative occupation of the allowed empty lattice bands geometrically in $k$-space [7]. The entire Fermi surface has a constant energy $E_F$ in the momentum space. In other words, it is the surface, where all fermions state with momentum $k < k_F$ is occupied and other higher momentum states are unoccupied. Any variation in the unoccupied states around the Fermi surface may lead to the generation of electrical current. Hence, the study of the Fermi surface topology is important to measure the electronic properties of the materials. The software XCrySDen [19] does the visualization of the Fermi surfaces. Figures 12 (a, b, c, d), show the Fermi surfaces for TiS$_2$. In the band structure of TiS$_2$, there are three bands are crossing the Fermi energy level $E_F$. The Fermi surface for individual bands passing through the $E_F$, are shown in Figures 12 (a, b, c). For merged bands, the Fermi surfaces are displayed in Figure 12 (d). The point-like concentric cylinders are at the zone center ($\Gamma$) and the quasi cylinders at the corners of the Brillouin zone in $\Gamma$-A direction give the electron contribution. The band in TiS$_2$ is shifted due to the electron-electron interaction of intercalated atom Cr with both Ti and S atoms.
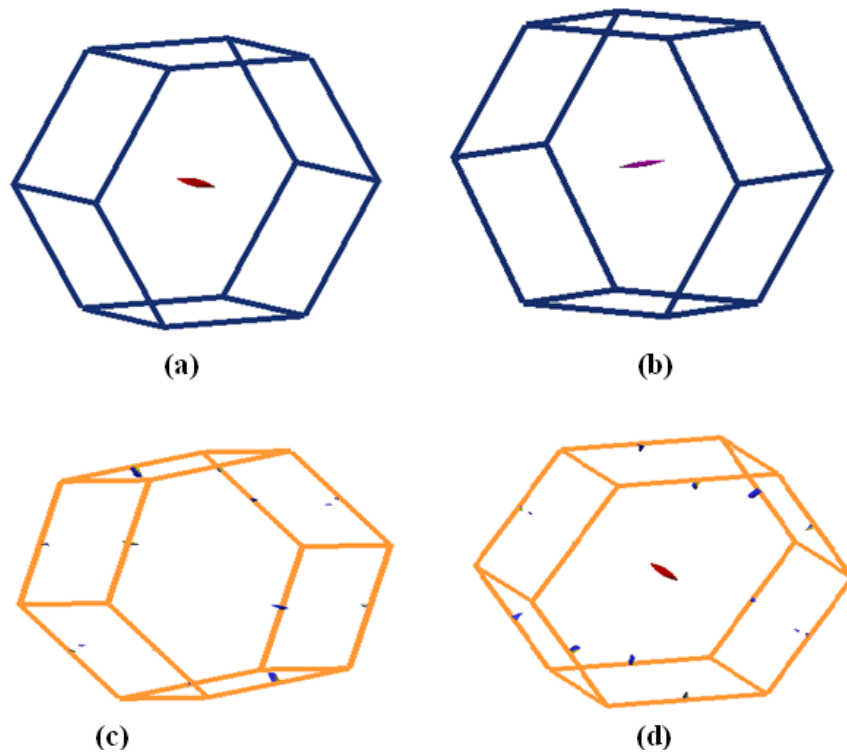


Figure 12. The Fermi surfaces of TiS$_2$ for different bands (a)-(c) and for merged band.

Figures 13 (a, b, c, d), display the Fermi surfaces for CrTiS$_2$ compounds. Here, there are three bands are crossing the Fermi energy level $E_F$. The Fermi surface for individual bands passing through the $E_F$, are shown in Figures 13 (a, b, c). For merged bands, the Fermi surfaces are displayed in Figure 13 (d). The hole-like concentric cylinders are seen at the zone center ($\Gamma$) and the quasi cylinders at the corners of the Brillouin zone in $\Gamma$-A direction give the electron contribution.
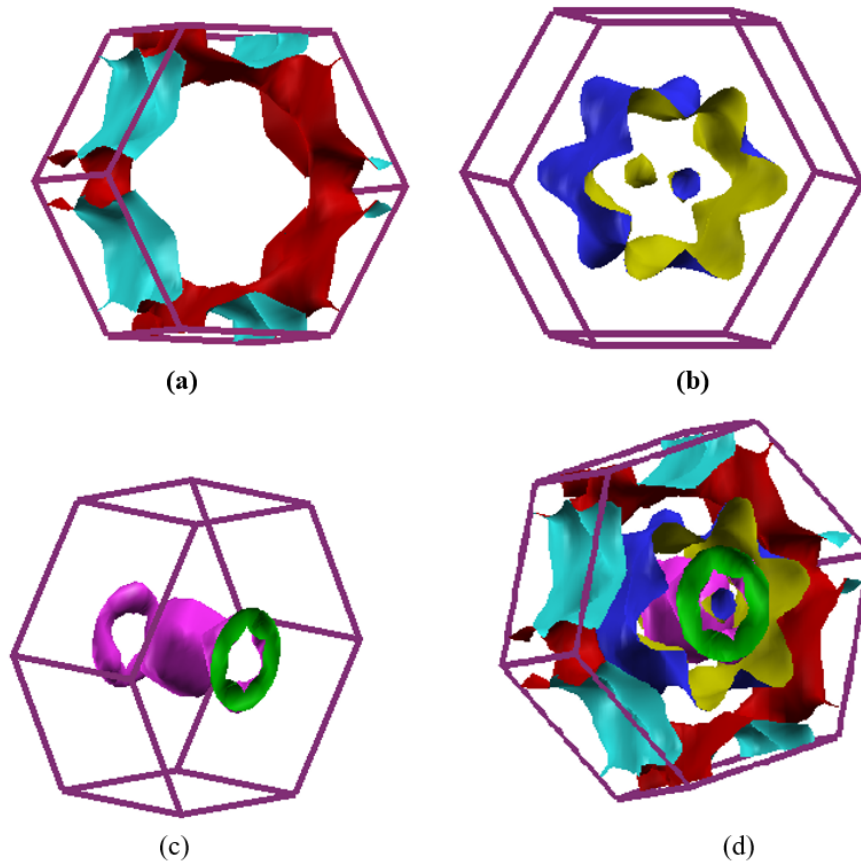
Figure 13. The Fermi surfaces of CrTiS2 for different bands (a) – (c) and for merged band (d).

# Conclusion

In this work, we carried out the DFT based simulation, supported by Kohn-Sham equation [22], was conducted using the plane wave code i.e. Quantum ESPRESSO [13] to investigate the structural analysis like lattice constants, electronic properties visualized electronic band structure, total and projected density of states (TDOS and PDOS) and the Fermi surfaces of intercalant compounds $TiS_2$ and $CrTiS_2$, by using GGA [14], including the exchange correlation effects with the functional proposed by PBE [15]. In structural optimization, the Cr atom is placed between $TiS_2$ interlayer. In electronic band structure, the $TiS_2$ has a small indirect bandgap or semi metallic band structure while it doping with Cr atom then there is change in the band structure is observed. The $CrTiS_2$ has an overlapping conduction band and valance band then the metallic structure. The Cr is a paramagnetic material. Same band structure is observed for spin up and spin down [12]. While, Sharma et al. [6] have reported different band structures for spin up and spin down by adopting the Wien2k code. But in the present case, we have not seen such type of nature in band structure results. For TDOS and PDOS in $TiS_2$ and $CrTiS_2$, at Fermi energy level, Cr 3d and Ti 3d-states are mainly contributed in the conduction band, where the S 2p-states contribute mainly to the valance band. The TDOS and PDOS of $TiS_2$ are near to zero at Fermi energy level while those for $CrTiS_2$ is maximum of 8.1 states/eV at the Fermi energy region. The Fermi surfaces corresponding to the energy

bands are intersecting at the Fermi level, in the band structure of $CrTiS_2$, the electron contribution can be easily detected. In $TiS_2$, the electron contribution is minimum because the energy band is not overlapping in the Fermi region. The electron contribution is maximum in $CrTiS_2$ at point M and K.

## Acknowledgements

## References

[1] N. Suzuki et al., J De Physique, Solid State Phys. C **8** (1998) 49201.
[2] T. Matsushita et al., Phys. Rev. B **60** (1999) 1678.
[3] Y. Ueda et al., Solid State Comm. **57** (1986) 839.
[4] Y-S. Kim et al., Mat. Trans. Jim. **8** (2000) 1088.
[5] Q. Yan-Bin et al., Phys. Lett. **24** (2007) 1050.
[6] Y. Sharma et al., Adv. Mater. Lett. **6**(4) (2015) 294-300.
[7] V.B. Zala et al., AIP Conference proceedings **2100** (2019) 020027.
[8] V.A. Dabhi et al., AIP Conference Proceedings **2224**(1) (2020) 030003.
[9] H.S. Patel et al., Springer proceedings in physics **236** (2019) 389-395.
[10] H.S. Patel et al., AIP Conference Proceedings **2224**(1) (2020) 030006.
[11] V.B. Parmar and A.M. Vora, East Eur. J. Phys. **1** (2021) 93-98.
[12] T. Yamasaki et al., J. Phys. C: Solid State Phys. **20** (1987) 395.
[13] P. Giannozzi et al., J. Phys. Condens. Matter **21** (2009) 395502.
[14] J.P. Perdew et al., Phys. Rev. B **48** (1993) 4978.
[15] J.P. Perdew et al., Physical Review Letters **77** (1996) 3865.
[16] http://www.quantum-espresso.org/pseudopotential.
[17] P.K. Janert, Gnuplot in action: understanding data with graphs.
[18] P.K. Janert, Journal of cheminformatics **3** (2011) 1.
[19] A. Kokalj, Journal of Molecular Graphics and Modelling **17** (1999) 176-179.
[20] C.M. Fang et al., Phys. Rev. B **56** (1997) 4455.
[21] Q. Yan-Bin et al., Phys. Lett. **24** (2007) 1050.
[22] W. Kohn and L.J Sham, Phys Rev. A**140** (1965) 1133.